



Original Research Article

Bioinformatic prediction and functional characterization of human KIAA0100 gene



He Cui^{a,1}, Xi Lan^{b,1}, Shemin Lu^b, Fujun Zhang^b, Wanggang Zhang^{a,*}

^a Department of Clinical Hematology, Affiliated No. 2 Hospital, Xi'an Jiaotong University, No. 157 West Five Road, Xi'an, Shaanxi 710004, China

^b Department of Biochemistry and Molecular Biology, School of Basic Medical Sciences, Xi'an Jiaotong University Health Science Center, No. 76 Yanta West Road, Xi'an, Shaanxi 710061, China

ARTICLE INFO

Keywords:

Human KIAA0100 gene
Bioinformatic prediction
Acute monocytic leukemia associated antigen
CRISPR/Cas9 system
Cell proliferation
Cell apoptosis

ABSTRACT

Our previous study demonstrated that human KIAA0100 gene is a novel acute monocytic leukemia-associated antigen (MLAA) gene. But the functional characterization of human KIAA0100 gene has remained unknown to date. Here, firstly, bioinformatic prediction of human KIAA0100 gene was carried out using online software; Secondly, human KIAA0100 gene expression was downregulated by the clustered regularly interspaced short palindromic repeats (CRISPR)/CRISPR-associated (Cas) 9 system in U937 cells. Cell proliferation and apoptosis were next evaluated in KIAA0100-knockdown U937 cells. The bioinformatic prediction showed that human KIAA0100 gene was located on 17q11.2, and human KIAA0100 protein was located in the secretory pathway. Besides, human KIAA0100 protein contained a signal peptide, a transmembrane region, three types of secondary structures (alpha helix, extended strand, and random coil), and four domains from mitochondrial protein 27 (FMP27). The observation on functional characterization of human KIAA0100 gene revealed that its downregulation inhibited cell proliferation, and promoted cell apoptosis in U937 cells. To summarize, these results suggest human KIAA0100 gene possibly comes within mitochondrial genome; moreover, it is a novel anti-apoptotic factor related to carcinogenesis or progression in acute monocytic leukemia, and may be a potential target for immunotherapy against acute monocytic leukemia.

1. Introduction

Acute myeloid leukemia (AML) is an aggressive blood cancer caused by the proliferation of immature myeloid cells [1]. Acute monocytic leukemia is a distinct subtype of AML, classified by the French-American-British (FAB) Classification as M₅ and often accompanied by specific chromosomal translocations, such as t (11;17) (q23;q21) [2], t (11;17) (q23;q25) [3], t (11;17) (q23;q12) [4], t (11;17) (q24;q21) [5], t (11;17) (123;q11-21) [6], t (9;11) (p22;q24) [5], t (9;11) (p22;q23) [7], t (9;11) (q33;q23) [8], t (11;20) (p15;q11.2) [9], t (11;20) (p15;q11) [10], t (1;11) (p31;q23) [11], t (1;11;4) (q21;q23;p16) [12], t (8;16) (p11;p13) [13], t (8;22) (p11;q13) [14], t (X;10) (p10;p10) [15], and others [16–18]. AML-M₅ can lead to hyperleukocytosis [19], extramedullary involvement [20], and coagulation abnormalities including disseminated intravascular coagulation [21]. It has been considered to be incurable so far. Thus, new methods of treatment are urgently needed.

Cancer immunotherapy is a therapeutic approach to harness the body's own immune system to fight cancer, and has begun to

demonstrate promising results in cancer patients since Coley [22] observed inoperable sarcoma shrinkage and even disappearance due to the injection of the mixed toxins of erysipelas and bacillus prodigiosus in and around tumours in the late nineteenth century. Allogeneic bone marrow transplantation and monoclonal antibodies that target tumor cells are two broadly-used examples of efficacious immunotherapies for leukemia [23].

We have been studying the immunotherapy of the acute leukemia since 1995, and have prepared vaccine by using inactivated autologous leukemia cells combined with interleukin-2 (IL-2), granulocyte-macrophage colony-stimulating factor (GM-CSF), and IL-6. Our study found that this new vaccine was feasible, safe, and capable of eliciting immune responses against leukemia, especially for AML-M₅ [24]. Moreover, the serologic analysis of recombinant cDNA expression library (SEREX) showed that human KIAA0100 gene was a novel acute MLAA gene, named as MLAA-22 [25], whose mRNA was highly expressed in newly diagnosed patients with AML-M₅ [26].

Peer review under responsibility of Xi'an Jiaotong University.

* Corresponding author.

E-mail address: zhangwanggang2003@yahoo.com (W. Zhang).

¹ These authors contributed equally to this work.

Human KIAA0100 belongs to the Human Unidentified Gene-Encoded (HUGE) database [27–30], which consists of over 2400 novel human genes obtained from the cDNA libraries of human fetal brain, adult whole brain, amygdale, hippocampus and cultured human immature myeloid cell line KG-1 [31–36]. Human KIAA0100 gene was identified from a cDNA library of human immature myeloid cell line KG-1 in the Kazusa cDNA sequencing project in 1995 [31]. The biological function of human KIAA0100 gene has still been unknown up to now.

Bioinformatics is a new multidisciplinary science, and can be applied in the cancer studies and therapies for many beneficial reasons [37]. In this study, based on nucleotide and predicted amino acid sequence of human KIAA0100, bioinformatic prediction was made by using online software with the aim to guide the research of human KIAA0100 gene's function.

The CRISPR/Cas9 system has been proven to be an efficient gene-editing tool for genome modification of cells and organisms [38]. It consists of two essential components, Cas9, an RNA-guided DNA double-strand endonuclease (RGEN), and a small guide RNA (sgRNA) that binds to, directs and programs Cas9 to cleave a nucleotide stretch of DNA through base-complementarity, so long as the targeted region is preceded by a short protospacer adjacent motif (PAM) sequence [39] (Fig. 1). The CRISPR/Cas9 system's ability to perturb the genome in a precise and targeted manner is crucial to understanding genetic contributions to biology and disease [40–42]. In this study, human KIAA0100 gene expression was down-regulated by the CRISPR/Cas9 system. The efficiency of sgRNAs was tested by suveyor assay, cell proliferation was evaluated by means of CCK-8, cell apoptosis assay was conducted by flow cytometry, and morphological changes of cell apoptosis were determined using Hoechst 33258 fluorescence staining.

2. Materials and methods

2.1. Materials

Rabbit polyclonal antibody against human KIAA0100 was purchased from Biorbyt Ltd. (Cambridge, Britain). Mouse anti- β -actin monoclonal antibody, RPMI-1640 medium, and enhanced chemiluminescence (ECL) reagents were purchased from Thermo Fisher Scientific Inc. (Waltham, USA). Horseradish peroxidase (HRP)-conjugated goat anti-rabbit IgG antibody and HRP-conjugated goat anti-mouse IgG antibody were purchased from Proteintech Group, Inc. (Chicago, USA). Knockout and Mutation Detection Kit was purchased from Shanghai Genesci Medical Technology Co., Ltd. (Shanghai, China). PureLink Genomic DNA Mini Kit was purchased from Life Technologies

Corporation (Carlsbad, USA). DNA Gel Extraction Kit was purchased from TIANGEN Biotechnology Co., Ltd. (Beijing, China). Cell Counting Kit-8 (CCK-8) was purchased from 7 Sea Biotech (Shanghai, China). Annexin V Apoptosis Detection Kit was purchased from eBioscience (San Diego, USA). Fetal bovine serum was purchased from Invitrogen (Carlsbad, USA). Radio immunoprecipitation assay (RIPA) lysis buffer was purchased from Beyotime Institute of Biotechnology (Shanghai, China). Protease inhibitor was purchased from Roche Diagnostics (Mannheim, Germany).

2.2. Bioinformatic prediction

The mRNAs sequence alignments, chromosomal maps and phylogenetic tree were predicted with Ensembl database (http://asia.ensembl.org/Homo_sapiens/Gene/). The putative coding sequence was predicated using Open Reading Frame (ORF) Finder of biocomputing services of the National Center for Biotechnology Information (NCBI) (<http://www.ncbi.nlm.nih.gov/gorf/gorf.html>). Derived protein sequence was analyzed using the following bioinformatics tools: Compute pI/Mw for molecular weight and theoretical isoelectric point (pI) prediction (http://us.expasy.org/tools/pi_tool.html), InterProScan5 for signal peptides prediction (<http://www.ebi.ac.uk/Tools/pfa/iprscan5/>), TargetP for intracellular localization prediction (<http://www.cbs.dtu.dk/services/TargetP/>) [43], TMHMM Server version 2.0 for transmembrane helices in protein (<http://www.cbs.dtu.dk/services/TMHMM/>), SOPMA for secondary structures prediction (<http://npsa-pbil.ibcp.fr/>) [44], and SMART for the domains prediction (http://smart.embl-heidelberg.de/smart/list_genomes.pl).

2.3. Cell and cell culture

U937 cells were obtained from the Department of Hematology, the Second Affiliated Hospital, Xi'an Jiaotong university (China), and were cultured in RPMI-1640 medium supplemented with 10% fetal bovine serum at 37 °C in a humidified atmosphere containing 5% CO₂. In all experiments, cells were used in the log-growth phase.

2.4. Human KIAA0100 gene knockdown by CRISPR/Cas9 system

CRISPR/Cas9 system was composed of two recombinant lentivirus vectors, which were lentivirus-cas9-puro and lentivirus-sgRNA-EGFPMCS^{MCS}. Lentivirus-cas9-Puro carried puromycin resistance gene, and lentivirus-sgRNA-EGFPMCS^{MCS} was labeled with enhanced green fluorescent protein (EGFP). Three single guide RNAs (sgRNAs) targeting human KIAA0100 gene were designed and synthesized by Genechem Co., Ltd. (Shanghai, China). Lentivirus-cas9-puro vector and three lentivirus-sgRNA-EGFPMCS^{MCS} vectors were constructed by Genechem Co., Ltd. (Shanghai, China). The sgRNAs sequences are listed in Table 1.

Firstly, the cultured U937 cells were infected by lentivirus-cas9-puromycin. To obtain stable expression of Cas9 in U937 cells, at 72 h after infection, cells were selected with 2.0 μ g/mL puromycin for 48 h to kill the undelivered cells and Cas9-U937 cells were obtained. Secondly, the log-phase Cas9-U937 cells were infected by three lentivirus-sgRNA-EGFPMCS^{MCS} vectors, respectively. EGFP was observed using inverted fluorescence microscope at 72 h after infection with

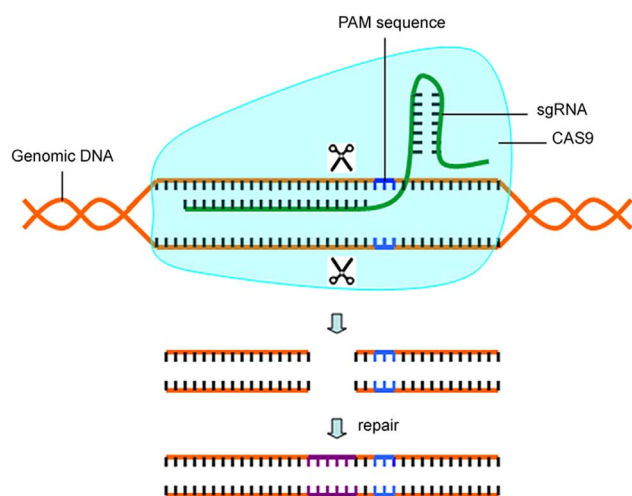


Fig. 1. The mechanism of targeted genome editing via CRISPR/Cas9 system.

Table 1
The sgRNAs sequences.

Number	sgRNA (5'–3')
KD1	CTGCAGCGGAGCTAAAGAT
KD2	GGAGTTTGCTGGAATCCAC
KD3	CACATGTGGCATTGTGCTT

Table 2

The primer sequences and enzyme digestion information needed for effective sgRNA screening.

Number	Primer sequence (5'–3')	Amplified fragment (bp)	Endonuclea fragement 1 (bp)	Endonuclea fragement 2 (bp)
KD1	F: GAGGCCAGGAAGTGAATAGGAG R: CCTGGACACTCTGTGCTCTACA	898	620	278
KD2	F: TTCAGGAACGACCTTTTGCAAGG R: GGGCAGACAGGTCAGAAACTTT	1050	645	405
KD3	F: TGATCTTCCGTGAGTACCCTAT R: TTAACACCTTGATAAGGAGGCC	830	325	505

lentivirus-sgRNA-EGFP^{MCS} and the percentage of green fluorescence-positive cells was calculated using flow cytometry.

2.5. Suveryor assay and TA clones sequencing

Suveryor assay was performed to test the lentivirus-sgRNA-EGFP^{MCS}'s cleavage by using Knockout and Mutation Detection Kit according to the manufacturer's instructions at 120 h after infection with lentivirus-sgRNA-EGFP^{MCS}, and the most effective sgRNA was picked out. Briefly, genomic DNA was extracted by using the PureLink Genomic DNA Mini Kit according to the manufacturer's instructions. PCR amplification program of sgRNAs target regions was next pre-denatured for 2 min at 95 °C, followed by 35 cycles of denaturation at 95 °C for 30 s, annealing at 55 °C for 30 s, extension at 72 °C for 60 s, and a final extension at 72 °C for 5 min, cooled to < 40 °C, and then finally separated by 1% agarose gel electrophoresis.

All PCR primers for suveryor assay are listed in Table 2. The PCR products of the most effective sgRNA target region were purified by DNA Gel Extraction Kit and cloned into pMDTM18-T vector with the pMDTM18-T vector cloning kit. A total of 31 positive clones were next sequenced by GenScript Co., Ltd, and human KIAA0100 gene mutation rate was evaluated.

2.6. Preparation of the total protein and Western blot analysis

The log-phase Cas9-U937 cells were infected by the most effective lentivirus-sgRNA-EGFP^{MCS}. The cells were washed twice with cold phosphate buffered saline (PBS) at 120 h after infection, and then lysed in cold RIPA lysis buffer and protease inhibitor for 30 min. The product was centrifuged at 14,000 *g* for 20 min at 4 °C. The supernatant was collected and stored in refrigerator at –80 °C. The total protein was next separated by 6% SDS-PAGE, and transferred onto nitrocellulose filter membrane. The membrane was blocked in 5% skim milk at room temperature for 2 h, and then incubated with primary antibody (Rabbit polyclonal antibody against human KIAA0100, 1:200) overnight at 4 °C, followed by HRP-conjugated goat anti-rabbit IgG antibody (1:5,000) at 27 °C for 1 h and 45 min. β -actin was blotted to show equal protein loading. The signals were developed using the ECL reagents, and specific protein bands were observed by using GeneGenome chemiluminescence imaging system (Syngene, Britain).

2.7. Proliferation assay

CCK-8 was used to detect the cell proliferation. The log-phase Cas9-U937 cells were infected by the most effective lentivirus-sgRNA-EGFP^{MCS}, at 16 h after infection, cells were plated on 96-well plates at the density of 2×10^3 cells per well and allowed to grow for 5 days after infection. 10 μ L CCK-8 solution was added into each well at harvest time. After incubation for 4 h at 37 °C in a humidified atmosphere containing 5% CO₂, the optical density (OD) value was recorded at 450 nm using a microplate reader (Bio-Rad, Richmond, USA). The experiment was performed in triplicates.

2.8. Cell apoptosis assay

The log-phase Cas9-U937 cells were infected by the most effective lentivirus-sgRNA-EGFP^{MCS}, at 120 h after infection, cell apoptosis assay was performed with Annexin V Apoptosis Detection Kit. Collected cells were washed twice in 4 °C PBS, and washed in 1 \times binding buffer. Cells were next resuspended by 200 μ L 1 \times binding buffer at a concentration of 1×10^6 cells/mL and added 10 μ L Annexin V-allophycocyanin (APC), and then incubated at room temperature for 15 min in dark. Before being analyzed by flow cytometry, another 400 μ L 1 \times binding buffer was added to the tube. Cells were finally analyzed by flow cytometry (BD Bio-sciences, Franklin Lakes, USA). The experiment was performed in triplicates.

2.9. Morphological study

The log-phase Cas9-U937 cells were infected by the most effective lentivirus-sgRNA-EGFP^{MCS}, at 120 h after infection, cells were collected and washed twice in 4 °C PBS, and stained with Hoechst 33258 staining solution according to the manufacturer's instructions (Beyotime, China). Cells were observed using inverted fluorescence microscope and scored as apoptotic if their nuclei presented chromatin condensation and marginalization or nuclear beading [45].

2.10. Statistical analysis

All data were expressed as mean \pm standard deviation (SD). The statistical analyses were performed using SPSS version 13.0 (SPSS, Inc., Chicago, IL, USA). Student's t-test was used to compare two groups of independent samples. $P < 0.05$ was considered statistically significant.

3. Results

3.1. Bioinformatic prediction

Human KIAA0100 gene was located on 17q11.2 (Fig. 2). Its coding region was 6708 bp. The mRNAs alignment among some species revealed that the mRNA sequence of human KIAA0100 gene had 99%, 91%, 90%, 90%, 90%, 90%, 88%, 88%, and 80% identity with that of chimpanzee KIAA0100 ortholog gene, *Sus scrofa* KIAA0100 ortholog gene, *Cavia porcellus* KIAA0100 ortholog gene, *Bos taurus* KIAA0100 ortholog gene, *Oryctolagus cuniculus* KIAA0100 ortholog gene, *Canis lupus familiaris* KIAA0100 ortholog gene, *Mus musculus* RIKEN cDNA 2610507B11 gene (2610507B11Rik), *Rattus norvegicus* similar to CG14967-PA (RGD1307929) gene and *gallus* KIAA0100 gene, respectively. The phylogenetic tree showed that the relationship between



Fig. 2. Human KIAA0100 gene was located on chromosome 17q11.2.

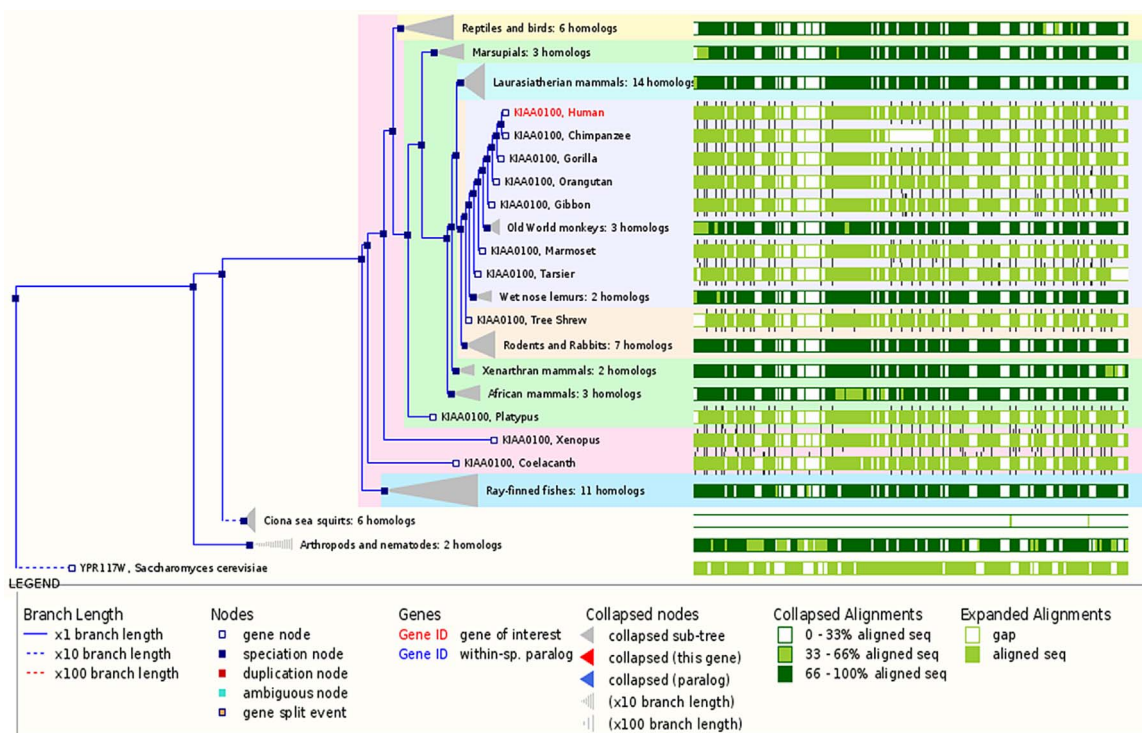


Fig. 3. The phylogenetic tree of human KIAA0100 gene. The phylogenetic tree showed that Human KIAA0100 gene and chimpanzee KIAA0100 gene were in a cluster, and their relationship was the closest.

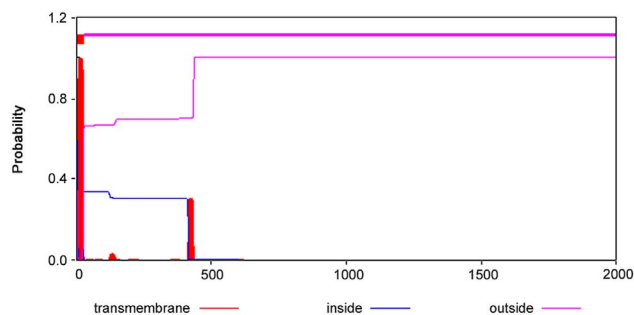


Fig. 4. The bioinformatic prediction of transmembrane regions of human KIAA0100 protein by TMHMM. The result showed that there was one predicted transmembrane region (5-SALLVLLLVALSALFLGRWL-27) in human KIAA0100 protein.

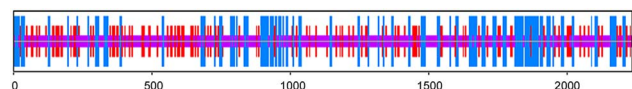


Fig. 5. Predicted secondary structures of the human KIAA0100 protein by SOPMA. The result showed that the human KIAA0100 protein contained three types of secondary structures, namely alpha helix (25.28%), extended strand (19.19%), and random coil (55.53%). Alpha helices, extended strands, random coils were indicated with the longest, the second longest, and the shortest vertical lines, respectively.

human KIAA0100 gene and chimpanzee KIAA0100 gene was the closest (Fig. 3). The open reading frame indicated that human KIAA0100 protein consisted of 2235 amino acid residues with a molecular weight of 254 Da and a PI of 6.71. Moreover, human KIAA0100 protein contained a predicted signal peptide (1-MPLFFSALLVLLLVALSALFLGRWL-29), a predicted transmembrane region (5-SALLVLLLVALSALFLGRWL-27) (Fig. 4). The intracellular localization prediction by TargetP showed that human KIAA0100 protein was located in the secretory pathway. In addition, the prediction of secondary structure by SOPMA showed that the human KIAA0100 protein included three types of secondary structures: alpha helix (25.28%), extended strand (19.19%), and random coil



Fig. 6. Predicted functional domains of human KIAA0100 protein by SMART. The result indicated that there were four predicted functional domains in human KIAA0100 protein, which were N-terminal of FMP27 (27aa–473aa), N-terminal of FMP27 (450aa–672aa), GFWDK domain of FMP27 (1028aa–1160aa), and C-terminal of FMP27 (1703aa–2176aa) in human KIAA0100 protein.

(55.53%) (Fig. 5). The domains prediction by SMART showed that there were four high probably domains: N-terminal of mitochondrial protein 27 (FMP27) (27aa–473aa), N-terminal of FMP27 (450aa–672aa), GFWDK domain of FMP27 (1028aa–1160aa), and C-terminal of FMP27 (1703aa–2176aa) in human KIAA0100 protein (Fig. 6).

3.2. Suveryor assay, TA clones sequencing, and Western blot analysis

We found the percentage of green fluorescence-positive cells was 92.5% (KD1-sgRNA), 94.6% (KD2-sgRNA), 93.4% (KD3-sgRNA) at 120 h after infection with three lentivirus-sgRNA-EGFP^{MCS}, respectively (Fig. 7). Genomic DNA was then isolated, the region surrounding the CRISPR target site was PCR amplified, and the product was screened by suveryor assay. Suveryor assay showed that the most effective sgRNA was KD2-sgRNA (Fig. 8). The purified PCR products of KD2-sgRNA target region were cloned into pMDTM18-T vector and sequenced. TA positive clones sequencing results indicated that there were 19 clones to develop mutation in 31 clones, and the human KIAA0100 gene mutation rate was 61.3% (Fig. 9). Western blot analysis demonstrated the KIAA0100 protein expression was obviously decreased in U937 cells by using CRISPR/Cas9 system (Fig. 10).

3.3. Human KIAA0100 gene downregulation inhibited the proliferation of U937 cells

To assess the function of human KIAA0100 protein in cell proliferation, CCK-8 assay was performed from the first day to the

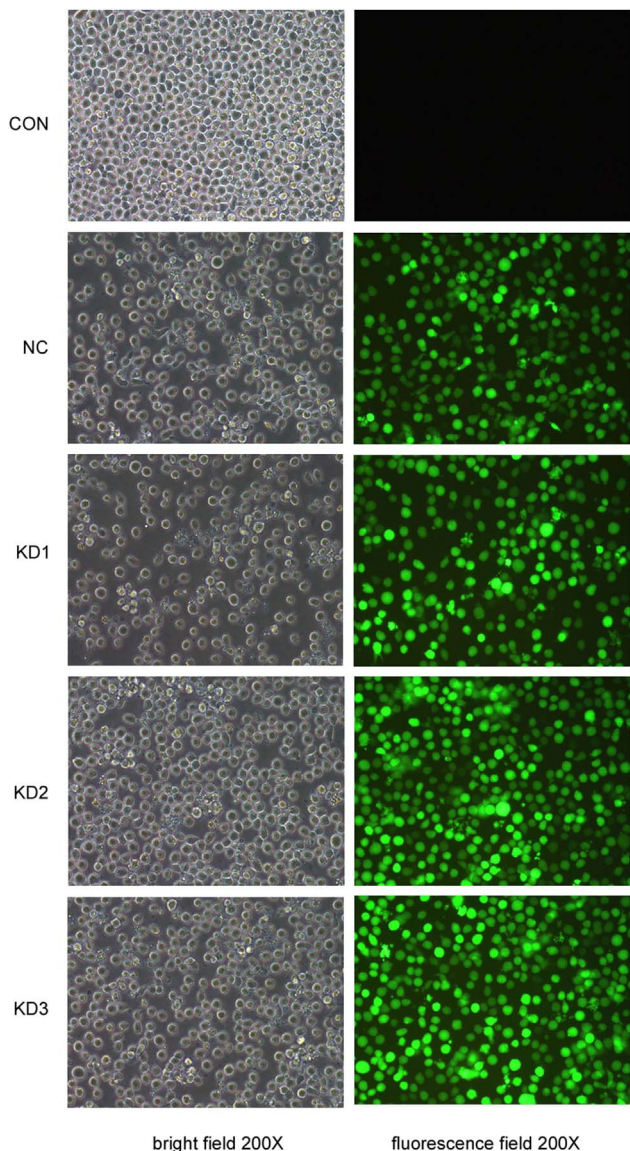


Fig. 7. Fluorescence Microscopy results of Cas9-U937 cells transduced with lentivirus-sgRNA-EGFP^{MCS}. The results showed the percentage of green fluorescence-positive cells was all over 90% at 120 h after infecting three lentivirus-sgRNA-EGFP^{MCS}. CON: blank control. NC: negative control. KD: knockdown.

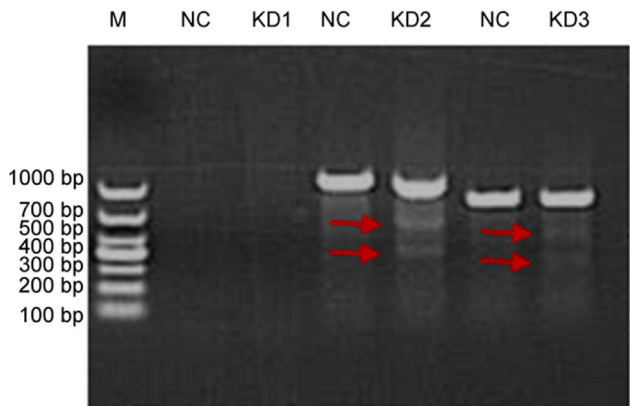


Fig. 8. Surveyor assay showed the most effective sgRNA was KD2 sgRNA. The red arrows indicated the expected positions of DNA bands cleaved by surveyor nuclease.



Fig. 9. TA clones sequencing data for the KIAA0100 targeting region in U937 cells. The 20-base pair (bp) target sequence was shown in red; the PAM sequence was shown in blue; the inserted nucleotides were shown in green; the displaced nucleotides were shown in orange; short black lines denoted different deletions. WT: wild type.

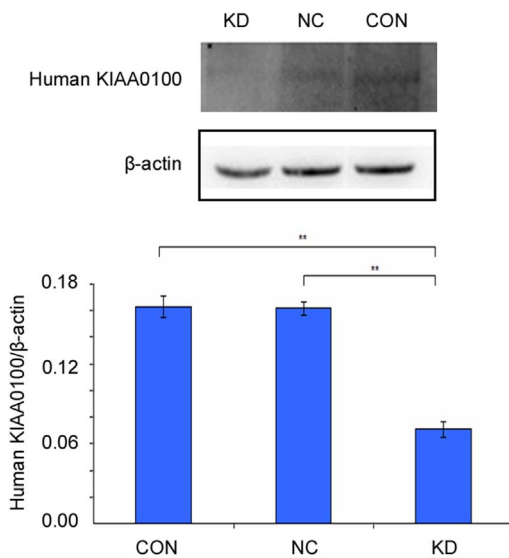


Fig. 10. Western blot analysis for the human KIAA0100-knockdown U937 cells. Western blot indicated the human KIAA0100 expression was lowest in KIAA0100-knockdown U937 cells. Data were displayed as mean \pm SD. ****** $P < 0.01$.

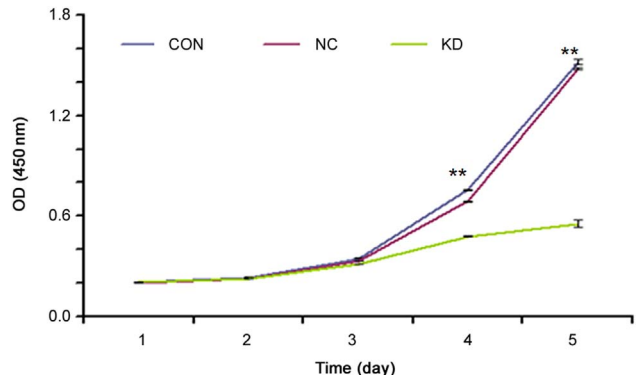


Fig. 11. Cell proliferation in KIAA0100-knockdown U937 cells. The result indicated that the KIAA0100-knockdown U937 cells grew more slowly than those in CON and NC on the fourth day and the fifth day after infection with lentivirus-KD2-sgRNA-EGFP^{MCS} ($P < 0.01$), and the difference was more pronounced with the time prolonged. The experiment was performed in triplicate and data were displayed as mean \pm SD. ****** $P < 0.01$.

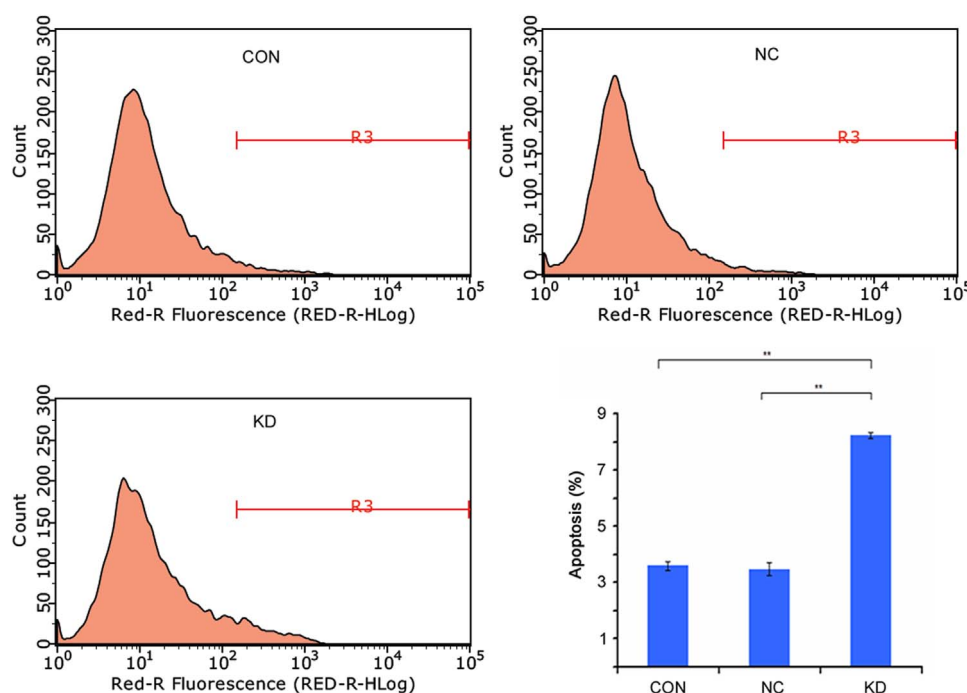


Fig. 12. Cell apoptotic in KIAA0100-knockdown U937 cells. The result showed the downregulation of human KIAA0100 gene increased the percentage of apoptotic cells. The experiments was performed in triplicate and data were displayed as mean \pm SD. $**P < 0.01$.

fifth day after infection with lentivirus-KD2-sgRNA-EGFP^{MCS}. The result indicated that the KIAA0100-knockdown U937 cells grew the most slowly ($P < 0.01$), and the difference was more pronounced with the prolonged time (Fig. 11).

3.4. Human KIAA0100 gene downregulation increased the apoptosis of U937 cells

To determine the mechanism responsible for human KIAA0100 gene downregulation mediated inhibition of U937 cells growth, apoptosis assay was conducted by flow cytometry. The results showed the apoptotic cells were $3.59\% \pm 0.14\%$ in blank control (CON), $3.47\% \pm 0.23\%$ in negative control (NC), and $8.23\% \pm 0.10\%$ in knockdown (KD). Moreover, the apoptotic cells were the most in KIAA0100-knockdown U937 cells ($P < 0.01$). These results confirmed that the downregulation of human KIAA0100 gene expression increased the percentage of apoptotic cells (Fig. 12).

3.5. Observation of morphological changes

To observe the morphological changes of cell apoptosis, human KIAA0100 gene knockdown U937 cells were stained with Hoechst 33258 staining solution. Under light microscopy, human KIAA0100 gene knockdown U937 cells showed morphological features such as chromatin condensation and marginalization (Fig. 13). Hoechst 33258 staining showed that there were significant morphological changes in the nuclear chromatin, and the nuclei were stained the brightest blue in the knockdown groups (Fig. 13). Apoptotic cells were $24.35\% \pm 3.82\%$ in CON, $18.82\% \pm 2.29\%$ in NC, and $18.82\% \pm 2.29\%$ in KD by Hoechst 33258 staining. Moreover, the apoptotic cells were the most in KIAA0100-knockdown U937 cells ($P < 0.01$). The morphological changes also verified that downregulation of human KIAA0100 gene expression increased the percentage of apoptotic cells.

4. Discussion

The identification of tumor antigens is a precondition of immunotherapy. In order to find new approaches to treat leukemia with

immunotherapy, the researchers have discovered some leukemia associated antigens (LAAs) last two decades, such as Wilms tumor-1 (WT1) [46–48], proteinase 1 [49,50], BCR-ABL fusion gene [51,52], Aurora-A kinase [53,54], MLAA-34 [25,55–58], etc. Some immunotherapy drugs targeted these LAAs have entered clinical trials.

Our previous SEREX analysis found that human KIAA0100 gene was a novel acute monocytic leukemia-associated antigen (MLAA) gene, also named MLAA-22 [25], and in addition to that, we also observed its mRNA expression was present with a high number of copy messages in AML-M₅ by quantitative real-time PCR. However, the functional characterization of human KIAA0100 gene has remained unknown to date.

Breast cancer-overexpressed gene 1 (BCOX1), an alternative splicing variant of human KIAA0100 gene, whose predicted open reading frame of 666 bp could encode a protein of 222 amino acid residues with a calculated molecular weight of 24.920 kDa, and whose mRNA expression moderately elevated in ductal in situ carcinoma (DCIS), peaked in invasive breast carcinoma (IBC) and metastatic breast carcinoma cells (MET), but absent in benign ductal epithelial cells [59]. Furthermore, high level of BCOX1 expression was associated with poor prognosis in patients with invasive ductal carcinomas of the breast [60]. In addition, microRNA-195 could suppress tumor cell proliferation and metastasis by directly targeting BCOX1 in prostate carcinoma [61].

In this study, bioinformatic predictive analysis indicated human KIAA0100 gene was located on 17q11.2. The mRNAs alignment among some species revealed that the mRNA sequence of human KIAA0100 gene was conserved in chimpanzee, *Sus scrofa*, *Cavia porcellus*, *Bos taurus*, *Oryctolagus cuniculus*, *Canis lupus*, *Mus musculus*, *Rattus norvegicus* and *Gallus*. The predicted KIAA0100 open reading frame of 6708 bp encoded a protein of 2235 amino acid residues with a calculated molecular weight of 254 Da and a PI of 6.71. Besides, human KIAA0100 protein contained a predicted signal peptide (1-MPLFFSALLVLLVLSALSALFLGRWLVRV-29), a predicted transmembrane region (5-SALLVLLVLSALSALFLGRWLVRV-27), three types of secondary structures (alpha helix, extended strand, and random coil). The intracellular localization prediction showed that human KIAA0100 protein was located in the secretory pathway. More significantly, the

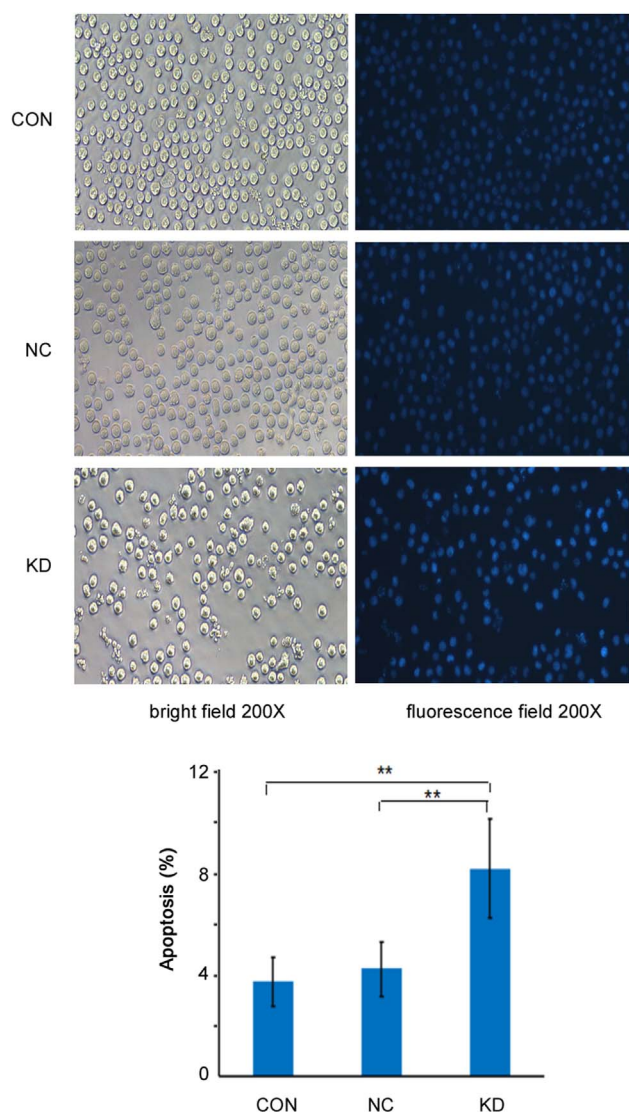


Fig. 13. U937 cells were stained with Hoechst 33258 detected and the apoptotic cells were calculated by fluorescent photomicrographs at 200 \times . The results showed the apoptotic cells were the most in KIAA0100-knockdown U937 cells. The experiment was performed in triplicate and data were displayed as mean \pm SD. $**P < 0.01$.

domains prediction showed that there were four highly probable domains from FMP27 in human KIAA0100 protein, which suggested human KIAA0100 protein possibly came within mitochondrial genomes. FMP27's function has been unknown up to now. Mitochondria serve as energy-producing organelles in eukaryotic cells. In addition to providing the energy supply for cells, the mitochondria are also involved in other processes, such as proliferation, differentiation, information transfer, and apoptosis, and play an important role in regulation of cell growth and the cell cycle [62]. The mitochondrion is multi-functional and involved in many diseases, and most cancer cells contain homoplasmic mutations in the mitochondrial genome [63].

To reveal the functions of human KIAA0100 gene, we adopted CRISPR/Cas9 system to downregulate human KIAA0100 gene's expression in U937 cells in this study. CRISPR/Cas systems provide adaptive immunity against viruses and plasmids by using CRISPR RNAs (crRNAs) to guide the silencing of invading nucleic acids in bacteria and archaea [64]. According to Cas protein's sequences and structures, CRISPR/Cas systems are classified into three Types (I, II and III) [64,65], and CRISPR/Cas9 system belongs to type II systems. CRISPR/Cas9 system consists of sgRNA (a crRNA) and Cas9. Cas9 is

thought to be the sole protein responsible for crRNA-guided silencing of foreign DNA in CRISPR/Cas9 system [64,66–68]. Owing to its customizable guide RNA (gRNA) design, its genomic specificity, its efficiency, and its ability for multiplexing, Cas9 and its variants have shown great potential in the generation of genetically modified cell lines and organisms, the interrogation of dynamic gene function, improved gene therapies, and other applications [69–73]. Cas9's affinity to the hairpin transactivating RNA segment of the sgRNA sequences enables its assembly into an active targeted nuclease, then the sgRNA and Cas9 protein form RNA-protein complexes to cut both strands of the DNA that can be repaired by non-homologous end joining (NHEJ). NHEJ can cause insertions or deletions in the DNA that can result in frame-shifting and disruption of the gene [74,75]. Here, we selected the most efficient sgRNA (KD-2 sgRNA), which successfully downregulated human KIAA0100 gene expression by CRISPR/Cas9 system. The results showed that the downregulation of human KIAA0100 gene expression suppressed the proliferation of U937 cells and increased the percentage of apoptotic cells in U937 cells. These data indicate that human KIAA0100 gene is a novel anti-apoptotic factor related to carcinogenesis or progression in acute monocytic leukemia.

5. Conclusion

This is the first report on the functional characterization of human KIAA0100 gene in the world. In the first place, the bioinformatic prediction showed that human KIAA0100 gene was located on 17q11.2, and human KIAA0100 protein was located in the secretory pathway. Besides, human KIAA0100 protein contained a signalpeptide (1-MPLFFSALLVLLLVALSALFLGRWLVVR-29), a transmembrane region (5-SALLVLLLVALSALFLGRWLV-27), three types of secondary structures (alpha helix, extended strand, and random coil), and four domains from FMP27. Secondly, the observation on functional characterization of human KIAA0100 gene revealed that its downregulation inhibited cell proliferation and promoted cell apoptosis in U937 cells. In conclusion, these results suggest that human KIAA0100 gene possibly comes within mitochondrial genomes; moreover, it is a novel anti-apoptotic factor related to carcinogenesis or progression in acute monocytic leukemia, and may be a potential target for immunotherapy against acute monocytic leukemia.

Acknowledgments

We acknowledge financial support from the National Natural Science Foundation of China (No. 081718110232).

References

- [1] R. Austin, M.J. Smyth, S.W. Lane, Harnessing the immune system in acute myeloid leukaemia, *Crit. Rev. Oncol.* 103 (2016) 62–77.
- [2] K. Suzukawa, S. Shimizu, N. Nemoto, et al., Identification of a chromosomal breakpoint and detection of a novel form of an mLL-AF17 fusion transcript in acute monocytic leukemia with t(11;17)(q23;q21), *Int. J. Hematol.* 82 (2005) 38–41.
- [3] T. Kurosu, K. Tsuji, M. Ohki, et al., A variant-type mLL/SEPT9 fusion transcript in adult de novo acute monocytic leukemia (M_{5b}) with t(11;17)(q23;q25), *Int. J. Hematol.* 88 (2005) 192–196.
- [4] S. Shekhter-Levin, S.M. Gollin, S.S. Kaplan, et al., Involvement of the mLL and RARalpha genes in a patient with acute monocytic leukemia with t(11;17)(q23;q12), *Leukemia* 14 (2000) 520–522.
- [5] G.W. Dewald, S.J. Morrison-DeLap, K.A. Schuchard, et al., A possible specific chromosome marker for monocytic leukemia: three more patients with t(9;11)(p22;q24) and another with t(11;17)(q24;q21), each with acute monoblastic leukemia, *Cancer Genet. Cytogenet.* 8 (1983) 203–212.
- [6] B.R. Reeves, H. Kempinski, K. Jani, et al., A case of acute monocytic leukemia with t(11;17) involving a rearrangement of mLL-1 and a region proximal to the RARA gene, *Cancer Genet. Cytogenet.* 74 (1994) 50–53.
- [7] M.O. Diaz, M.M. Le Beau, P. Pitha, et al., Interferon and c-ets-1 genes in the translocation (9;11)(p22;q23) in human acute monocytic leukemia, *Science* 231 (1986) 265–267.
- [8] M. Le Coniat, S.P. Romana, O. Bernard, et al., A novel translocation, t(9;11)(q33;q23) involving the HRX gene in an acute monocytic leukemia, *C.R. Acad. Sci. III* 316 (1993) 692–697.

- [9] N. Kakazu, I. Shinzato, Y. Arai, et al., Involvement of the NUP98 gene in a chromosomal translocation t(11;20)(p15;q11.2) in a patient with acute monocytic leukemia (FAB-M5b), *Int. J. Hematol.* 74 (2001) 53–57.
- [10] S. Chen, Y. Xue, Z. Chen, et al., Generation of the NUP98-TOP1 fusion transcript by the t(11;20)(p15;q11) in a case of acute monocytic leukemia, *Cancer Genet. Cytogenet.* 140 (2003) 153–156.
- [11] I. Nölle, B. Schlegelberger, N. Schmitz, et al., Acute monocytic leukemia with translocation t(1;11)(p31;q23): simultaneous staining of chromosomes and cell surface antigens, *Haematol. Blood Transfus.* 33 (1990) 145–149.
- [12] C.W. So, S.K. Ma, T.S. Wan, et al., Analysis of MLL-derived transcripts in infant acute monocytic leukemia with a complex translocation (1;11;4)(q21;q23;p16), *Cancer Genet. Cytogenet.* 117 (2000) 24–27.
- [13] T. Hanada, I. Ono, Y. Minosaki, et al., Translocation t(8;16)(p11;p13) in neonatal acute monocytic leukaemia, *Eur. J. Pediatr.* 150 (1991) 323–324.
- [14] I. Kitabayashi, Y. Aikawa, A. Yokoyama, et al., Fusion of MOZ and p300 histone acetyltransferases in acute monocytic leukemia with a t(8;22)(p11;q13) chromosome translocation, *Leukemia* 15 (2001) 89–94.
- [15] K.F. Wong, K.J. Hayes, Y.O. Huh, et al., Translocation (X;10)(p10;p10): a rare but nonrandom cytogenetic abnormality in acute leukemia of myeloid differentiation, *Cancer Genet. Cytogenet.* 86 (1996) 153–155.
- [16] M.D. Otero, N.J. Zeleznik-Le, V. Chinwalla, et al., Cytogenetic and molecular analysis of the acute monocytic leukemia cell line THP-1 with an mLL-AF9 translocation, *Genes Chromosomes Cancer* 29 (2000) 333–338.
- [17] T. Taki, M. Akiyama, S. Saito, et al., The MYO1F, unconventional myosin type 1F, gene is fused to mLL in Infant acute monocytic leukemia with a complex translocation involving chromosomes 7, 11, 19 and 22, *Oncogene* 24 (2005) 5191–5197.
- [18] M.D. Reis, I.D. Dubé, P.H. Pinkerton, et al., "Jumping" translocations involving band 3q13.3 in a case of acute monocytic leukemia, *Cancer Genet. Cytogenet.* 51 (1991) 189–194.
- [19] U. Creutzig, J. Ritter, M. Budde, et al., Early deaths due to hemorrhage and leukostasis in childhood acute myelogenous leukemia. Associations with hyperleukocytosis and acute monocytic leukemia, *Cancer* 60 (1987) 3071–3079.
- [20] L. Peterson, L.P. Dehner, R.D. Brunning, Extramedullary masses as presenting features of acute monoblastic leukemia, *Am. J. Clin. Pathol.* 75 (1981) 140–148.
- [21] P. Fenaux, C. Vanhaesbroucke, M.H. Estienne, et al., Acute monocytic leukaemia in adults: treatment and prognosis in 99 cases, *Br. J. Haematol.* 75 (1990) 41–48.
- [22] W.B. Coley, The treatment of inoperable sarcoma by bacterial toxins (the mixed toxins of the *Streptococcus erysipelas* and the *Bacillus prodigiosus*), *Proc. R. Soc. Med.* 3 (1910) 1–48.
- [23] W.J. Lesterhuis, J.B. Haanen, C.J. Punt, Cancer immunotherapy-revisited, *Nat. Rev. Drug Discov.* 10 (2011) 591–600.
- [24] W.G. Zhang, S.H. Liu, X.M. Cao, et al., A phase I clinical trial of active immunotherapy for acute leukemia using inactivated autologous leukemia cells mixed with IL-2, GM-CSF and IL-6, *Leuk. Res.* 29 (2005) 3–9.
- [25] G. Chen, W. Zhang, X. Cao, et al., Serological identification of immunogenic antigens in acute monocytic leukemia, *Leuk. Res.* 29 (2005) 503–509.
- [26] F.L. Zhou, W.G. Zhang, X. Meng, et al., Bioinformatic analysis and identification for a novel antigen MLAA-22 in acute monocytic leukemia, *J. Exp. Hematol. Chin. Assoc. Pathophysiol.* 16 (2008) 466–471.
- [27] M. Suyama, T. Nagase, O. Ohara, HUGE: a database for human large proteins identified by Kazusa cDNA sequencing project, *Nucleic Acids Res.* 27 (1999) 338–339.
- [28] R. Kikuno, T. Nagase, M. Suyama, et al., HUGE: a database for human large proteins identified in the Kazusa cDNA sequencing project, *Nucleic Acids Res.* 28 (2000) 331–332.
- [29] R. Kikuno, T. Nagase, M. Waki, et al., HUGE: a database for human large proteins identified in the Kazusa cDNA sequencing project, *Nucleic Acids Res.* 30 (2002) 166–168.
- [30] R. Kikuno, T. Nagase, M. Nakayama, et al., HUGE: a database for human KIAA proteins, a 2004 update integrating HUGEppi and ROUGE, *Nucleic Acids Res.* 32D (2004) 502–504.
- [31] T. Nagase, N. Miyajima, A. Tanaka, et al., Prediction of the coding sequences of unidentified human genes. III. The coding sequences of 40 new genes (KIAA0081-KIAA0120) deduced by analysis of cDNA from clonishuman cell line KG-1, *DNA Res.* 2 (1995) 37–43.
- [32] O. Ohara, T. Nagase, K. Ishikawa, et al., Construction and characterization of human brain cDNA libraries suitable for analysis of cDNA clones encoding relatively large proteins, *DNA Res.* 4 (1997) 53–59.
- [33] T. Nagase, R. Kikuno, O. Ohara, Prediction of the Coding Sequences of Unidentified Human Genes. XXII. The complete Sequences of 50 New cDNA Clones Which Code for Large Proteins, *DNA Res.* 8 (2001) 319–327.
- [34] T. Nagase, R. Kikuno, O. Ohara, Prediction of the coding sequences of unidentified human genes. XXI. The complete sequences of 60 new cDNA clones from brain which code for large proteins, *DNA Res.* 8 (2001) 179–187.
- [35] T. Nagase, M. Nakayama, D. Nakajima, et al., Prediction of the coding sequences of unidentified human genes. XX. The complete sequences of 100 new cDNA clones from brain which code for large proteins in vitro, *DNA Res.* 8 (2001) 85–95.
- [36] N. Nomura, N. Miyajima, T. Sazuka, et al., Prediction of the coding sequences of unidentified human genes. I. The coding sequences of 40 new genes (KIAA0001-KIAA0040) deduced by analysis of randomly sampled cDNA clones from human immature myeloid cell line KG-1, *DNA Res.* 1 (1994) 27–35.
- [37] B.P.K. Reddy, S. Srinivasarao, Bioinformatics-its challenges, *Int. Adv. Res. J. Sci. Eng. Technol.* 2 (2015) 130–132.
- [38] Y. Ma, B. Shen, X. Zhang, et al., Heritable multiplex genetic engineering in rats using CRISPR/Cas9, *PLOS One* 9 (2014) e89413.
- [39] A. Malina, C.J. Cameron, F. Robert, et al., PAM multiplicity marks genomic target sites as inhibitory to CRISPR-Cas9 editing, *Nat. Commun.* 6 (2015) 10124.
- [40] X. Han, Z. Liu, M.C. Jo, et al., CRISPR-Cas9 delivery to hard-to-transfect cells via membrane deformation, *Sci. Adv.* 1 (2015) e1500454.
- [41] P.D. Hsu, E.S. Lander, F. Zhang, Development and applications of CRISPR-Cas9 for genome engineering, *Cell* 157 (2014) 1262–1278.
- [42] K. High, P.D. Gregory, C. Gersbach, CRISPR technology for gene therapy, *Nat. Med.* 20 (2014) 476–477.
- [43] O. Emanuelsson, H. Nielsen, S. Brunak, et al., Predicting subcellular localization of proteins based on their N-terminal amino acid sequence, *J. Mol. Biol.* (4) (2000) 1005–1016.
- [44] C. Geourjon, G. Deléage, SOPMA: significant improvements in protein secondary structure prediction by consensus prediction from multiple alignments, *Comput. Appl. Biosci.* 6 (1995) 681–684.
- [45] S. Kasibhatla, G.P. Amarante-Mendes, D. Finucane, et al., Staining of suspension cells with hoechst 33258 to detect apoptosis, *CSH Protoc.* 3 (2006) 778–781.
- [46] C. Rosenfeld, M.A. Cheever, A. Gaiger, WTI in acute leukemia, chronic myelogenous leukemia and myelodysplastic syndrome: therapeutic potential of WTI targeted-therapies, *Leukemia* 17 (2003) 1301–1312.
- [47] V.F. Van Tendeloo, A. Van de Velde, A. Van Driessche, et al., Induction of complete and molecular remissions in acute myeloid leukemia by Wilms' tumor 1 antigen-targeted dendritic cell vaccination, *Proc. Natl. Acad. Sci. U.S.A.* 107 (2010) 13824–13829.
- [48] T. Kitawaki, N. Kadowaki, K. Fukunaga, et al., A phase I/IIa clinical trial of immunotherapy for elderly patients with acute myeloid leukaemia using dendritic cells co-pulsed with WTI peptide and zoledronate, *Br. J. Haematol.* 153 (2011) 796–799.
- [49] K. Rezvani, A.S. Yong, S. Mielke, et al., Leukemia-associated antigen-specific T-cell responses following combined PR1 and WTI peptide vaccination in patients with myeloid malignancies, *Blood* 111 (2008) 236–242.
- [50] K. Rezvani, PR1 vaccination in myeloid malignancies, *Expert Rev. Vaccin.* (7) (2008) 867–875.
- [51] R.E. Clark, I.A. Dodi, S.C. Hill, et al., Direct evidence that leukemic cells present HLA-associated immunogenic peptides derived from the BCR-ABL b3a2 fusion protein, *Blood* 98 (2001) 2887–2893.
- [52] J.M. Rojas, K. Knight, S. Watmough, et al., BCR-ABL peptide vaccination in healthy subjects: immunological responses are equivalent to those in chronic myeloid leukaemia patients, *Leuk. Res.* 35 (2011) 369–372.
- [53] T. Ochi, H. Fujiwara, M. Yasukawa, Aurora-A kinase: a novel target both for cellular immunotherapy and molecular target therapy against human leukemia, *Expert Opin. Ther. Targets* 13 (2009) 1399–1410.
- [54] K. Nagai, T. Ochi, H. Fujiwara, et al., Aurora kinase A-specific T cell receptor gene transfer redirects T lymphocytes to display effective antileukemia reactivity, *Blood* 119 (2012) 368–376.
- [55] P.Y. Zhang, W.G. Zhang, A.L. He, et al., Identification and functional characterization of the novel acute monocytic leukemia associated antigen MLAA-34, *Cancer Immunol. Immunother.* 58 (2009) 281–290.
- [56] W.J. Zhang, W.G. Zhang, P.Y. Zhang, et al., The expression and functional characterization associated with cell apoptosis and proteomic analysis of the novel gene MLAA-34 in U937 cells, *Oncol. Rep.* 29 (2013) 491–506.
- [57] J. Zhao, A. He, W. Zhang, et al., Quantitative assessment of MLAA-34 expression in diagnosis and prognosis of acute monocytic leukemia, *Cancer Immunol. Immunother.* 60 (2011) 587–597.
- [58] L. Qian, W. Zhang, P. Zhang, et al., The anti-apoptosis effect of MLAA-34 in leukemia and the β -catenin/T cell factor 4 protein pathway, *Am. J. Transl. Res.* 7 (2015) 2270–2278.
- [59] J. Song, W. Yang, Ie.M. Shih, et al., Identification of BCOX1, a novel gene overexpressed in breast cancer, *Biochim. Biophys. Acta* 2006 (1760) 62–69.
- [60] T. Liu, X.Y. Zhang, X.H. He, et al., High levels of BCOX1 expression are associated with poor prognosis in patients with invasive ductal carcinomas of the breast, *PLOS One* 9 (2014) e86952.
- [61] J. Guo, M. Wang, X. Liu, MicroRNA-195 suppresses tumor cell proliferation and metastasis by directly targeting BCOX1 in prostate carcinoma, *J. Exp. Clin. Cancer Res.* 34 (2015) 91–98.
- [62] M. Wu, A. Kalyanasundaram, J. Zhu, Structural and biomechanical basis of mitochondrial movement in eukaryotic cells, *Int. J. Nanomed.* 8 (2013) 4033–4042.
- [63] S. Ohta, A multi-functional organelle mitochondrion is involved in cell death, proliferation and disease, *Curr. Med. Chem.* 10 (2003) 2485–2494.
- [64] M. Jinek, K. Chylinski, I. Fonfara, et al., A programmable dual-RNA-guided DNA endonuclease in adaptive bacterial immunity, *Science* 337 (2012) 816–821.
- [65] K.S. Makarova, L. Aravind, Y.I. Wolf, et al., Unification of Cas protein families and a simple scenario for the origin and evolution of CRISPR-Cas systems, *Biol. Direct* 6 (2011) 38.
- [66] R. Barrangou, C. Fremaux, H. Deveau, et al., CRISPR provides acquired resistance against viruses in prokaryotes, *Science* 315 (2007) 1709–1712.
- [67] J.E. Garneau, M.È. Dupuis, M. Villion, et al., The CRISPR/Cas bacterial immune system cleaves bacteriophage and plasmid DNA, *Nature* 468 (2010) 67–71.
- [68] R. Sapranaukas, G. Gasiunas, C. Frenaux, et al., The streptococcus thermophilus CRISPR/Cas system provides immunity in *Escherichia coli*, *Nucleic Acids Res.* 39 (2011) 9275–9282.
- [69] W. Zhou, A. Deiters, Conditional control of CRISPR/Cas9 function, *Angew. Chem. Int. Ed. Engl.* 55 (2016) 5394–5399.
- [70] A. Strauß, T. Lahaye, Zinc fingers, TAL effectors, or Cas9-based DNA binding proteins: what's best for targeting desired genome loci?, *Mol. Plant.* 6 (2013) 1384–1387.

- [71] L.A. Gilbert, M.H. Larson, L. Morsut, et al., CRISPR-mediated modular RNA-guided regulation of transcription in eukaryotes, *Cell* 154 (2013) 442–451.
- [72] M.H. Larson, L.A. Gilbert, X. Wang, et al., CRISPR interference (CRISPRi) for sequence-specific control of expression, *Nat. Protoc.* 8 (2013) 2180–2196.
- [73] L.S. Qi, M.H. Larson, L.A. Gilbert, et al., Repurposing CRISPR as an RNA-guided platform for sequence-specific control of gene expression, *Cell* 152 (2013) 1173–1183.
- [74] M. Yang, L. Zhang, J. Stevens, et al., CRISPR/Cas9 mediated generation of stable chondrocyte cell lines with targeted gene knockouts; analysis of aggrecan knockout cell line, *Bone* 69 (2014) 118–125.
- [75] P.D. Hsu, E.S. Lander, F. Zhang, Development and applications of CRISPR-Cas9 for genome engineering, *Cell* 157 (2014) 1262–1278.